ARTICLE

Integrating envirotyping and genetic modeling to dissect crossover G×E interaction and stability in maize

Marcos Antonio de Godoy Filho[1*], Michael Keith Butterfield[2], Maurício dos Santos Araújo[1], José Tiago Barroso Chagas[1] and José Baldin Pinheiro[1]

Crop Breeding and Applied Biotechnology
26(1): e54682613, 2026
Brazilian Society of Plant Breeding.
Printed in Brazil
http://dx.doi.org/10.1590/1984-70332026v26n1a3

Abstract: *Genotype × environment (G×E) interaction is a primary challenge in plant breeding. This study integrates envirotyping with genetic modeling to dissect G×E for maize yield using the Genomes to Fields dataset. We utilized PaCMAP dimensionality reduction to classify 272 environments into four target populations of environments, which segregated into two mega-environments (Southern and Northern U.S.). A strong crossover interaction was detected between these mega-environments, resulting in low performance stability (quantified by the S index), primarily driven by an inverse relationship between growing degree days and silking, as well as yield: longer-cycle hybrids were advantageous in the South, while shorter-cycle hybrids excelled in the North. Our findings provide quantitative evidence that this phenological response, linked to photoperiod sensitivity, is a key mechanism underlying the G×E interaction. This framework offers a robust tool for defining breeding targets and accelerating genetic gain.*

Keywords: Zea mays *L., adaptation, factor analytic, enviromics, mega-environment*

INTRODUCTION

Genotype × environment (G×E) interaction is a primary challenge in quantitative genetics and plant breeding, occurring when different genotypes respond distinctly to environmental variations (Falconer and Mackay 1996, Pereira et al. 2025). This interaction can manifest in two forms: simple, when it arises from differences in the magnitude of genetic variances across environments, and crossover, when the genetic covariances between pairs of environments are low or negative, resulting in changes in the ranking of genotypes (Cooper and DeLacy 1994).

These changes in ranking stem from specific interactions between genotypes and environmental conditions during plant development, such that climatic, edaphic, and management features can be incorporated into the modeling of these interactions (Jarquín et al. 2014, Resende et al. 2021, Costa-Neto et al. 2021a, Cooper et al. 2022, Araújo et al. 2024). As crossover interaction represents one of the most significant challenges within a breeding program, developing methodologies capable of modeling and exploiting G×E is of paramount importance to maximize genetic gains and identify germplasm adapted to different environmental conditions.

***Corresponding author:**
E-mail: marcos.a.godoy.f@gmail.com

Received: 14 November 2025
Accepted: 03 December 2025
Published: 17 December 2025

[1] Escola Superior de Agricultura Luiz de Queiroz, Departamento de Genética, Avenida Pádua Dias, 11, 13418-900, Piracicaba, SP, Brazil
[2] Centro de Tecnologia Canavieira, Fazenda Santo Antonio, s/n, 13400-970, Piracicaba, SP, Brazil

An advance in the understanding of G×E was introduced by Cooper and DeLacy (1994), who proposed decomposing the interaction variance into components associated with changes in scale (non-crossover) and changes in the ranking of genotypes (crossover). The dissemination of linear mixed models (LMMs) in plant breeding represented a methodological improvement, enabling the modeling of variance and covariance structures between pairs of environments, such as compound symmetry, unstructured model, and Factor Analytic (FA) (Smith et al. 2001, 2005). The last-mentioned method gained popularity due to its ability to estimate the variance-covariance matrix with fewer parameters than an unstructured model. In this approach, genetic effects are captured by linear combinations of a reduced number of latent factors, which in turn capture the principal patterns of genotypic response (Crossa et al. 2004, Smith et al. 2005). However, mixed models describe the existence of G×E patterns, but do not explain why they occur. This limitation is overcome through the integration of envirotyping, which involves the systematic characterization of environmental variation and its incorporation into genetic-statistical models (Jarquín et al. 2014, Araújo et al. 2024).

This process involves quantifying environmental covariates (ECs), such as temperature, precipitation, ecophysiological features, and soil texture. ECs can be used for various purposes, such as defining Target Populations of Environments (TPEs), aiding in genomic prediction for untested locations, and interpreting the latent factors of FA analyses (Costa-Neto et al. 2021a, Araújo et al. 2025, Cruz et al. 2025). The combination of multi-environment trials (METs), factor analytic modeling, and envirotyping establishes a practical toolkit that allows for the understanding of G×E patterns and the identification of genotypes with broad or specific adaptation, enabling the optimization of resource allocation, such as the selection of representative test locations, and increasing selection accuracy through the exploitation of the interaction.

This study leverages the extensive Genomes to Fields (G2F) dataset to implement an integrated framework for dissecting G×E interactions in maize. The primary objective is to utilize high-resolution envirotyping, integrating detailed climatic data across phenological windows, to classify trial locations into data-driven TPEs. We employ a combination of nonlinear dimensionality reduction and clustering algorithms to achieve this classification. The primary objective of this research is to determine whether those TPEs effectively partition the crossover component of G×E for grain yield, as quantified through FA mixed models. Beyond partitioning the interaction, a further objective is to elucidate the biological drivers of the observed G×E patterns. We hypothesize that differential responses in phenology, specifically the relationship between Growing Degree Days (GDD) to silking and grain yield, are a key feature of hybrid adaptation within and across the identified TPEs.

MATERIAL AND METHODS

Phenotypic data and adjusted genotypic values

The phenotypic data originate from the G2F Initiative, a large-scale, public-private collaborative consortium that provides results from a network of METs in the United States. This work utilized the phenotypic dataset containing records for grain yield (Mg ha^{-1}) at the plot level and days to silking, which was transformed into GDD to silking. The data were collected in field trials conducted between 2014 and 2023 and comprise a total of 272 environments (location-year combinations) and 341 trials (Genomes to Fields 2025). Each trial was analyzed individually for yield and degree days to silking using linear mixed models (LMMs) with *ASReml-R* (Butler et al. 2023). To accommodate the diversity of experimental designs, the model structure was dynamically adjusted:

For trials with a randomized complete block design (RCBD), the fitted model was:

$$Y_{ij} = \mu + G_i + R_j + \epsilon_{ij}$$

where Y_{ij} is the observed phenotype, μ is the overall mean, G_i is the fixed effect of the ith hybrid, R_j is the fixed effect of the jth replication, and ϵ_{ij} is the random residual error, assumed as $\epsilon_{ij} \sim N(0, \sigma^2_e)$.

For trials with an incomplete block design, the model was expanded to:

$$Y_{ijk} = \mu + G_i + R_j + B_{k(j)} + \epsilon_{ijk}$$

where $B_{k(j)}$ represents the fixed effect of the kth block nested within the jth replication, allowing for finer control of local spatial variation. For incomplete blocks with convergence issues or non-estimable empirical Best Linear Unbiased Estimates (eBLUEs) due to severe imbalance, a fallback strategy was employed, consisting of fitting a complete block model.

For each trial, from an analogous model where the hybrid effect was considered random ($G_i \sim N(0, \sigma^2_g)$), the broad-sense heritability was estimated: (H^2):

$$H^2 = \frac{\sigma^2_g}{\sigma^2_g + (\sigma^2_\epsilon / r_h)}$$

where σ^2_g is the genotypic variance, σ^2_ϵ is the residual variance, and r_h is the harmonic mean of the number of replications of the hybrids. The experimental coefficient of variation (CV_e) was also calculated from σ^2_ϵ and the grain yield mean $\overline{Y}$.

$$CV_e = \frac{\sqrt{\sigma^2_\epsilon}}{\overline{Y}}$$

When the same environment included more than one trial, a joint analysis was performed, considering the fixed effect of the experiment and its nested structures (replications and blocks), to capture systematic variations between experiments conducted in the exact location and year.

Environmental characterization

Creating a climatic profile for each environment required defining a unique and representative temporal window that encompassed the crop growth cycle. In the dataset, 86 environments contained two or more trials, which required an evaluation of the variability in management dates. The mean planting interval between experiments within the same environment was only one day, with 75% of the environments showing no difference. For harvesting, consistency was maintained, with a mean interval of 2.4 days and 75% of the environments exhibiting a difference of less than 2 days. Due to the consistency of dates, the mean planting date and mean harvest date were calculated for each of the 86 environments with more than one experiment. That measure defines the start and end points for extracting daily meteorological data from the NASA POWER database. The *EnvRtype* package was used to calculate agrometeorological features, and a total of 33 environmental features were accessed (Costa-Neto et al. 2021b).

The crop growth cycle was partitioned into two macrophases, vegetative and reproductive, delimited by days to silking and normalized by GDD. The vegetative phase windows were defined as fractions of the total GDD accumulated from planting to silking, resulting in the following segmentation: W1 (from planting to 40% of the GDD to silking), W2 (from 40% to 90%), and W3 (from 90% to 100%). Subsequently, the reproductive phase windows were defined as fractions of the total GDD accumulated between silking and harvest, as follows: W4 (from silking to 10% of the reproductive GDD), W5 (from 10% to 30%), W6 (from 30% to 65%), and W7 (from 65% to the end of the growth cycle). The features were then summarized by the mean within each window, resulting in a matrix of environmental covariates.

The matrix of environmental covariates was subjected to the nonlinear dimensionality reduction technique PaCMAP (Pairwise Controlled Manifold Approximation) with n_neighbors = 6, MN_ratio = 0.5, and FP_ratio = 4, as developed by Wang et al. (2021), to describe the interrelationships among the environments. Each environment was represented as a point in a three-dimensional space defined by the PaCMAP components derived from the climatic variables across phenological windows. The *k*-means clustering algorithm was then applied to the PaCMAP components to test K clusters, where each cluster represents a TPE; the number of TPEs was defined by the Caliński and Harabasz (1974) methodology.

Validation of the TPEs

To validate whether the TPEs are capable of capturing crossover G×E interaction for grain yield, the data were filtered to include only hybrids present in at least 20 environments and with an occurrence in a minimum of five environments within each TPE, resulting in a dataset of 92 hybrids evaluated in 168 environments. For GDD to silking, only environments with grain yield data were considered, and the analysis was restricted to hybrids present in at least four environments in each TPE, totaling 86 hybrids in common with the dataset used for yield, evaluated in 130 environments.

These data were subjected to an FA model with different numbers of latent factors (K=2 up to 5 for yield, 1 up to 2 for GDD to silking):

$$Y_{ij} = \mu + e_j + (Ge)_{ij} + \epsilon_{ij}$$

where Y_{ij} is the eBLUE of the i^{th} hybrid in the j^{th} environment, obtained from the first-stage; μ is the overall mean; e_j represents the random effect of the j^{th} environment, assuming the distribution $e_j \sim N(0, \sigma^2_e)$; $(Ge)_{ij}$ corresponds to the

random effect of the interaction between the i[th] hybrid and the j[th] environment, assuming $(Ge)_{ij} \sim N(0, \sigma^2_{ge})$; and ϵ_{ij} is the residual error, weighted by $w_{ij} = 1/[\sigma^2(eBLUE_{ij})]$.

The G×E interaction was decomposed by means of a factor analytic structure:

$$(Ge)ij = \sum_{k=1}^{K} \lambda_{jk} f_{ik} + \delta_{ij}$$

where λ_{jk} represents the factor loading of the j[th] environment on the k[th] latent factor, f_{ik} is the factor score of the i[th] hybrid, and δ_{ij} is the environment-specific term not explained by the factors.

The optimal number of factors was determined based on the total variance explained by the factorial structure, adopting a threshold of 80% as the criterion (Smith and Cullis 2018). After fitting, the factor loadings (Λ) were subjected to orthogonal rotation via singular value decomposition (SVD). The genetic covariance matrix between environments (Σ_G) was reconstructed using the equation:

$$\Sigma_G = \Lambda\Lambda' + \Psi,$$

where Ψ is the diagonal matrix of environment-specific variances not explained by the factors. From Σ_G the genetic correlation matrix was derived, which was then explored to infer the degree of genetic consistency between environments belonging to the same TPE.

Stability across TPEs

Hybrid stability across TPEs was estimated based on the consistency of the mean performance rankings of the hybrid in each environmental group. For each hybrid, the ranking within each TPE was calculated based on the mean of the Empirical Best Linear Unbiased Predictor (eBLUPs). Subsequently, the stability index *S* was defined, which quantifies the relative change in rank of each hybrid across TPEs.

The S_i metric was calculated as:

$$S_i = 1 - \frac{|\bar{R}_{ij} - \bar{R}_i|}{N}$$

where R_{ij} is the rank of hybrid *i* in TPE *j*, $\bar{R}_i$ is the mean rank of the genotype across TPEs, $|\bar{R}_{ij} - \bar{R}_i|$ is the mean absolute deviation of the ranks, and *N* is the total number of hybrids. *S* values close to 1 indicate greater stability (lower rank variation across TPEs), while lower values reflect greater instability. The relationship between responsiveness (mean of the G×E interaction effects) and stability (S_i) was explored through a bivariate plot, allowing the identification of hybrids with simultaneously high and predictable performance across TPEs.

Relationship between GDD to silking and yield

The predicted values of yield and GDD to silking, obtained from the fitted FA models, were used to describe the relationship between both traits within each TPE. Only environments that contained observations for both traits were considered, ensuring direct correspondence between the datasets. For each TPE, a first-degree locally weighted regression (LOESS) was applied between the predicted values of yield and GDD to silking, in order to capture the functional structure and potential nonlinear patterns of the association between the traits within each environmental context.

RESULTS AND DISCUSSION

Characterization of the Target Populations of Environments (TPEs)

Following the dimensionality reduction of the climatic dataset via PaCMAP, the Caliński and Harabasz (1974) index was calculated, which reached its maximum value at k = 4, indicating that this is the optimal number of TPEs, offering the best balance between within-cluster cohesion and between-cluster separation. The visualization of the four TPEs is presented in Figure 1. The 3D scatter plot, generated by the PaCMAP technique, represents each environment as a point in space, where the proximity between points reflects the similarity of their climatic profiles. Coloring by the four TPEs defined by the k-means algorithm reveals a spatial separation of the groups. The geographical distribution of the TPEs, overlaid on a map of the United States' Agroecological Zones, is presented in Figure 1. The analysis reveals distinct

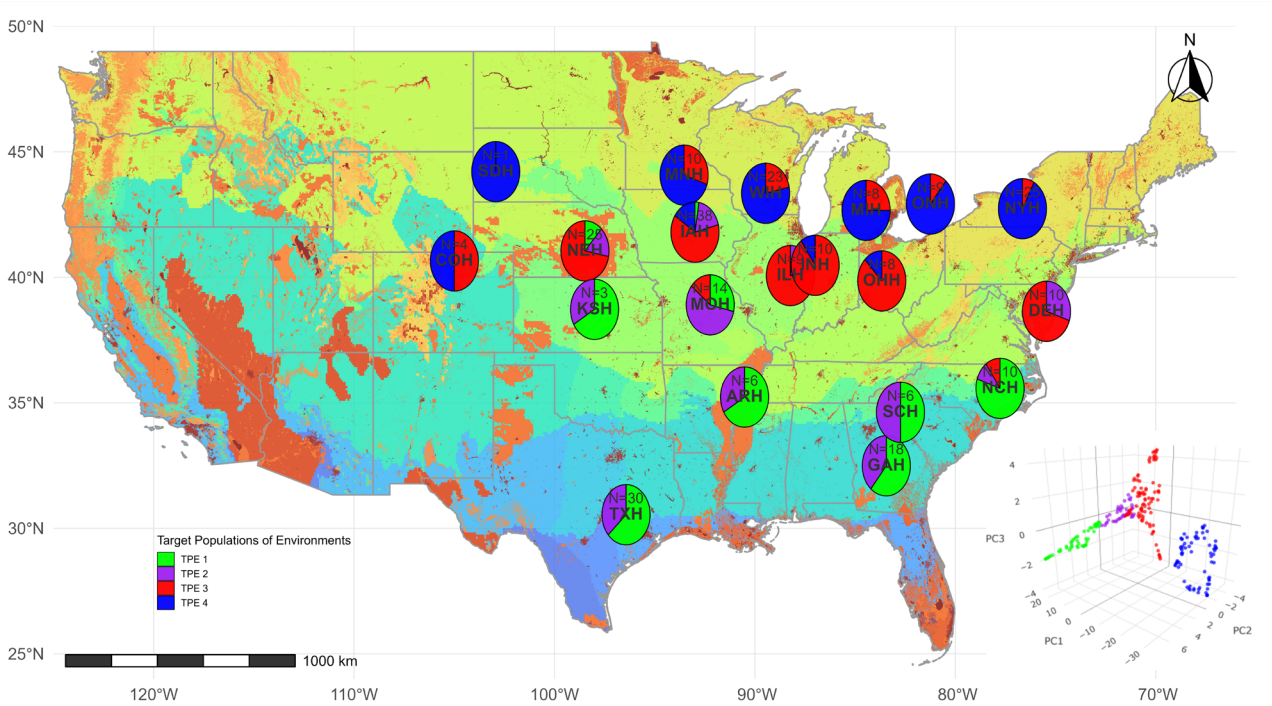

Figure 1. Map of the Agroecological Zones of the United States (FAO 2025), showing the trial locations. The pie charts at each location indicate the proportion of environments classified into each of the four TPEs, revealing distinct geographical distribution patterns. N is the number of environments. Adjacent is a 3D scatter plot generated from the nonlinear components of PaCMAP, where each point represents one environment.

spatial patterns that align with the major agricultural regions and climatic gradients, indicating that the TPEs represent mega-environments with specific management and yield characteristics.

TPEs 1 and 2 are consistently located in the southern portion of the country. These environments are characterized by the lowest mean yields (8.38 and 8.22 Mg ha^{-1}, respectively). This lower performance is associated with an earlier planting window, which extends from March to May. Specifically, TPE 1 concentrates the plantings in April (56% of environments), whereas TPE 2 has a more balanced distribution between April (34%) and May (44%).

In contrast, TPEs 3 and 4 are more concentrated in the central and northern regions, encompassing a large part of the Corn Belt area. Those TPEs represent the environments with the highest production potential and mean yields (10.40 and 10.04 Mg ha^{-1}, respectively). Management in those locations is characterized by later and more concentrated plantings. Approximately 80% of the environments in TPE 3 and 68% in TPE 4 have planting conducted in May, with some extending into June. This later planting window is a strategy to avoid spring frosts and capitalize on the ideal summer temperature and solar radiation conditions in the northern and midwestern United States, thereby maximizing yield potential.

The TPEs show sensitivity in capturing not only geographical differences but also interannual climatic variability and the impact of planting dates within a specific location. This capability is clear in Wisconsin (WIH), where 23 environments were distributed between TPE 3 and TPE 4. Despite the general predominance of TPE 4 in this location, all environments conducted in 2023 were classified as TPE 3, evidencing the capture of a strong year effect. Within the same year, as in 2021, the management effect was also distinct. Of the three environments evaluated, the trial with planting in April was classified as TPE 4, whereas the other two, with planting in May, were grouped into TPE 3, isolating the impact of the planting date on the environmental profile.

Similar patterns of annual variation are observed in several other locations. In Texas (TXH), the TPEs captured the distinction between the years 2021 and 2023, where both years had three environments, but each year was grouped

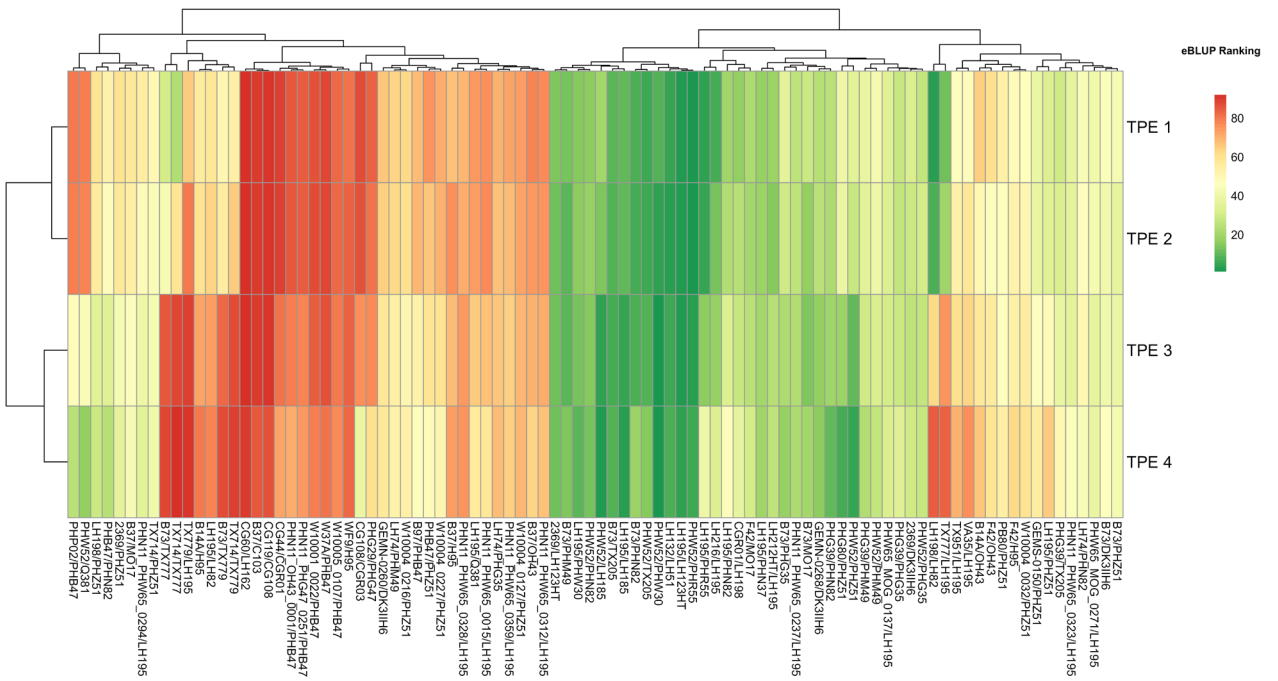

Figure 2. Yield ranking of the hybrids across the TPEs. Colors range from green (best-ranked) to red (worst-ranked), and the dendrogram on the Y-axis groups the hybrids based on the similarity of their response patterns.

into different TPEs (1 and 2). In this location, it was also possible to isolate the effect of planting date; in 2017, an environment with late planting in May was classified as TPE 1, while three other environments with earlier plantings in March and April were characterized as TPE 2.

These examples demonstrate the capability of envirotyping to differentiate the effects of location, year, and the interaction between year and management (planting date), consolidating these sources of variation into distinct clusters. This is a direct result of characterizing environments at the resolution of individual trials rather than as static geographical locations. By enabling the disentanglement of these complex spatio-temporal effects, the resulting clear separation between northern and southern mega-environments not only validates this high-resolution classification but also corroborates the broad spatial patterns identified by Lopez-Cruz et al. (2023).

Genetic correlations

The analysis of the G×E interaction for grain yield was performed on the filtered dataset, comprising 92 hybrids evaluated in 168 environments. The decomposition of the G×E interaction revealed that a model with two latent factors (FA2) was sufficient to capture the underlying structure of the yield patterns and interactions. This model explained 83.39% of the total variance.

The mean genetic correlation matrix between and within the TPEs, derived from the FA2 model, is presented in Figure 5. The genetic correlations within each TPE, represented on the diagonal of the matrix, revealed moderate to high values, ranging from 0.60 (TPE 2) to 0.75 (TPE 4). These coefficients indicate a high level of consistency in the ranking of the hybrids within each group, validating the effectiveness of the clustering in forming environmentally homogeneous groups.

The analysis of the hierarchical structure of the correlations, visualized by the dendrogram, revealed a clear segregation of the TPEs into two distinct mega-environments. The first was composed of TPEs 1 and 2, which exhibited a strong genetic association with each other (0.63). The second mega-environment, comprising TPEs 3 and 4, also showed a high internal correlation (0.66) (Figure 5).

The primary source of crossover G×E interaction was evidenced by the low genetic correlation between these two mega-environments. The most pronounced contrast was observed between TPE 4 and TPEs 1 and 2, where the correlation coefficients were reduced to 0.34 and 0.43, respectively (Figure 5). Values of this magnitude indicate a substantial change in the ranking of the hybrids, implying that the selection of hybrids based on performance in one mega-environment would be ineffective for predicting their behavior in the other.

The visualization of the crossover G×E interaction is presented in the heatmap of Figure 2, which displays the ranking of the 92 hybrids in each of the four TPEs. The hierarchical analysis of the hybrids (Y-axis) revealed the formation of distinct groups with specific adaptation patterns, confirming the mega-environment structure identified by the correlation matrix. A group of hybrids, located in the upper portion of the heatmap, showed superior performance in TPEs 3 and 4, which correspond to the high-potential environments of the Corn Belt; these same hybrids showed consistently lower performance in TPEs 1 and 2. It is also possible to identify hybrids with the opposite adaptation pattern, showing better adaptation to the southern environments than to the northern ones. Three of these stand-out hybrids originate from the Texas inbred line TX777. Additionally, some hybrids with high stability are observed, consistently ranking among the best or worst in all TPEs.

Stability and silking

For an integrated analysis of the performance and stability of the hybrids, a scatter plot was generated relating mean responsiveness (eBLUP) to ranking stability (*S* index) across the TPEs; S is based on the nonparametric methodology of Huehn (1990). This approach enables the classification of hybrids into four quadrants with distinct adaptation profiles (Figure 3). The upper-right quadrant of the plot identifies the most desirable hybrids, which combine high responsiveness (eBLUP > 0) and high stability (*S* > 0.92) (Figure 3). A significant number of hybrids are located in this region, characterizing them as materials with high performance and broad adaptability, consistently exhibiting superior performance in the majority of TPEs. In contrast, the lower-right quadrant groups hybrids with high responsiveness but low stability. Hybrids such as PHW52/LH185 and LH195/PHR55 belong to this group, indicating that, although their mean performance is

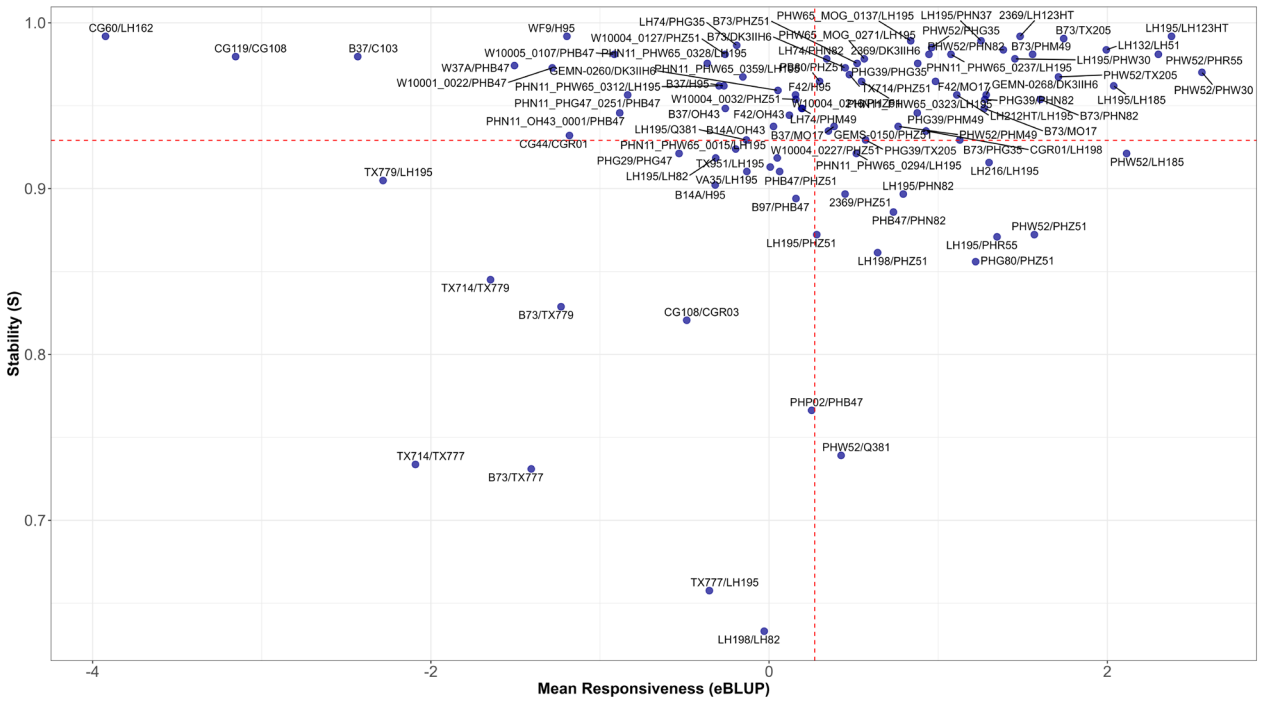

Figure 3. Scatter plot of Mean Responsiveness (eBLUP) versus Ranking Stability index (S). The upper-right quadrant contains the most desirable hybrids, characterized by high performance and stability across all TPEs.

high, their ranking can vary significantly across the TPEs. Other hybrids with mean performance near the population average, such as TX777/LH195 and LH198, have lower stability but can still excel under specific conditions; in the case of these two hybrids, they excel in TPEs 1 and 2.

The modeling of silking revealed a simpler interaction pattern, with a single factor explaining 91.25% of the interaction, indicating a predominance of simple interactions, as previously evidenced by He et al. (2025) with data from the Genomes to Fields initiative. The analysis of the relationship between grain yield and GDD to silking reveals that phenology is a determining factor for the adaptation and stability of the hybrids, being one of the factors that impact the crossover G×E and the stability observed between the North and South mega-environments (Figure 4). In the environments of the southern region (TPE 1 and TPE 2), which have a mean thermal accumulation to silking of 796 GDD and 776 GDD, respectively, the yield response curve demonstrates an advantage for longer-cycle hybrids, where maximum yield is achieved by hybrids that silk with a GDD near 800 and remains relatively stable up to 900 GDD, particularly in TPE 1. In contrast, shorter-cycle (early) hybrids are consistently penalized with lower yield.

Although TPEs 3 and 4 exhibit a mean GDD to silking within a similar range (792 GDD and 733 GDD, respectively), they show an opposite pattern. In these higher-yielding environments, the response curve favors shorter-cycle hybrids, with peak yield occurring within a GDD window of 775-825 in TPE 3 and 720-770 GDD in TPE 4, which predominantly comprises the northernmost environments. Hybrids that exceed these thresholds, particularly in TPE 4, experience a sharp decline in yield.

Hybrids with an intermediate cycle to silking are those that exhibit the highest stability and are the most numerous, suggesting a form of stabilizing selection, as these are the hybrids that have been extensively tested across the most diverse environments of the entire dataset. This observed difference between hybrids adapted to the North and the South is explained by Drouault et al. (2025), who demonstrated the division in the response of temperate and tropical

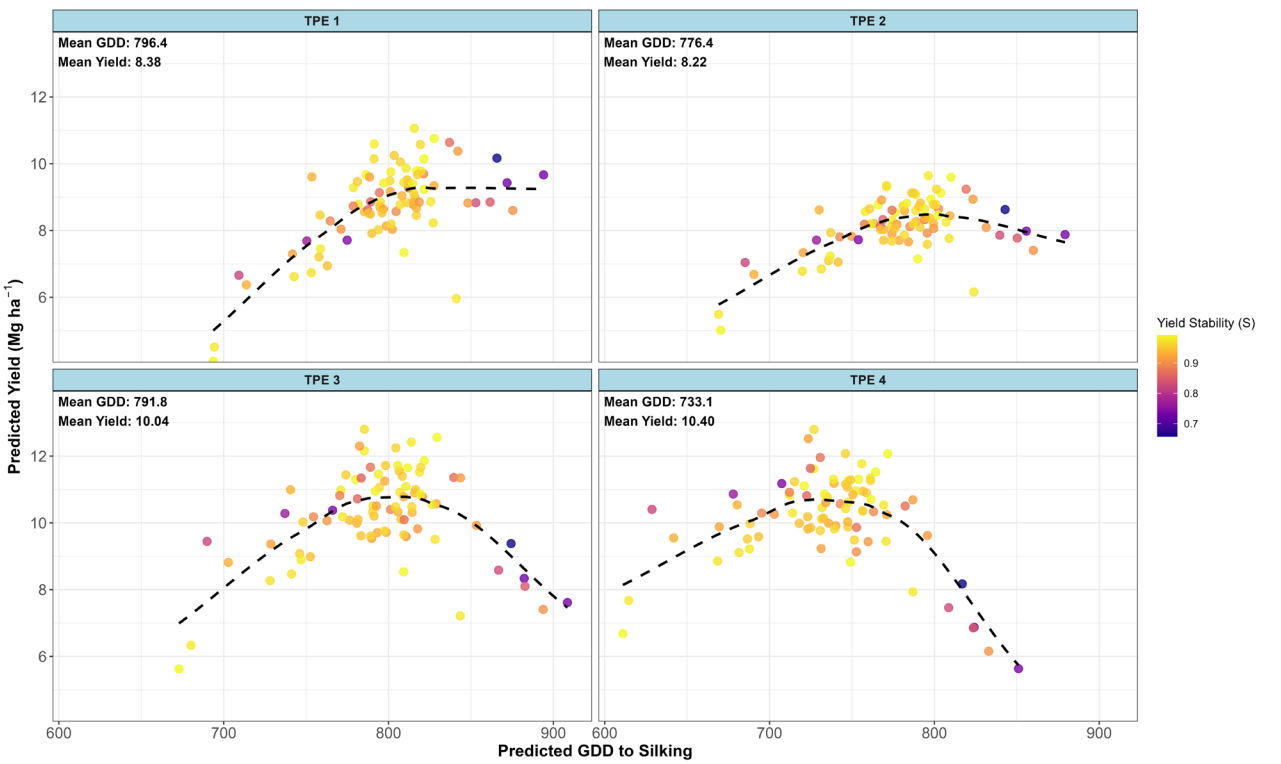

Figure 4. Predicted grain yield as a function of GDD to silking across the four TPEs. Each point is a hybrid colored by its yield stability (S) (yellow = high, purple = low). Dashed lines indicate LOESS regression trends

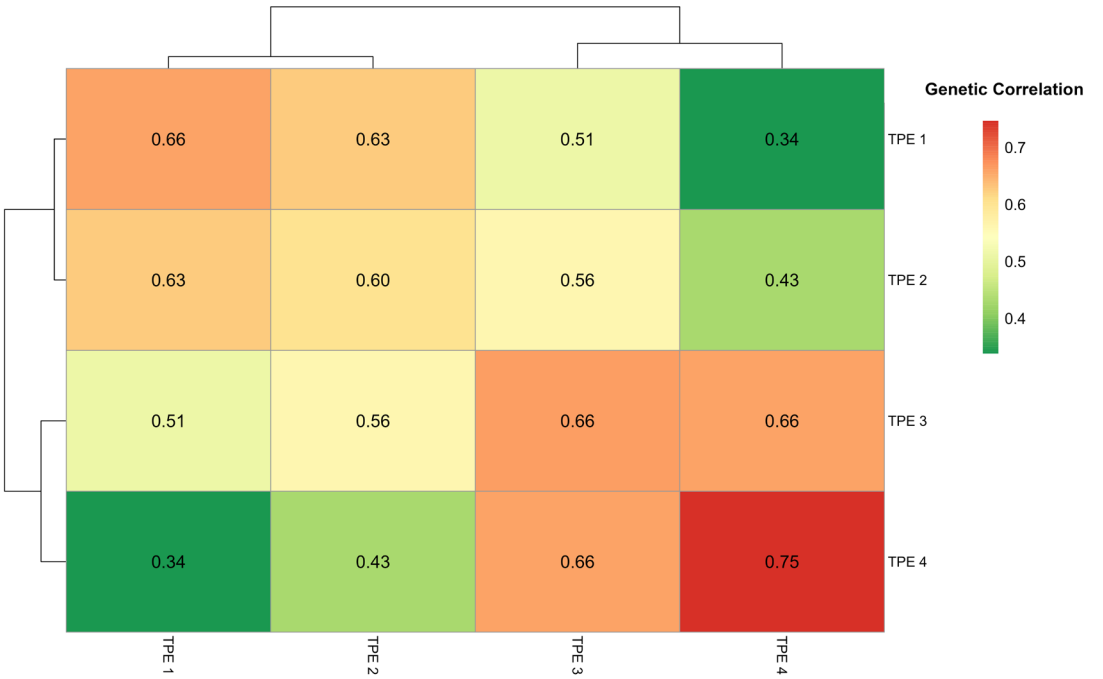

Figure 5. Genetic correlation matrix from the FA2 model for grain yield among the TPEs. The diagonal of the matrix shows the genetic correlations within each TPE. The off-diagonal values represent the genetic correlations between TPEs.

maize. The physiological mechanism underlying this division is photoperiod sensitivity, which acts as a flowering delay signal and is activated by long days. Temperate germplasm, corresponding to the hybrids with superior performance in the North, achieves its earliness by having been selected for low sensitivity, thereby ignoring the inhibitory signal of long days. In contrast, tropical germplasm, as well as the hybrids adapted to the South, maintains high sensitivity, and its silking is delayed under long days (Drouault et al. 2025).

CONCLUSIONS

This study demonstrates the efficacy of an integrated enviromics framework for dissecting complex G×E patterns in maize. The application of the nonlinear dimensionality reduction technique PaCMAP proved highly efficient in condensing high-dimensional climatic data into a meaningful, low-dimensional representation of the environmental space. This enables achieving the goal of classifying environments into four distinct TPEs, which were subsequently validated by their ability to effectively partition the crossover component of G×E for grain yield. The success of this data-driven approach underscores the value of incorporating detailed environmental characterization into genetic analyses, moving beyond simply describing G×E patterns to elucidating their underlying environmental drivers.

The segregation of environments into two distinct mega-environments provided strong quantitative evidence that phenological adaptation is a primary determinant of yield performance and stability. This differential adaptation was explicitly captured by the stability index, which quantified the instability arising from the strong crossover interaction. Hybrids with an intermediate flowering cycle showed the highest stability across all TPEs, whereas those adapted to the phenological extremes of either mega-environment were inherently unstable when evaluated across the entire environmental network. This finding directly links the physiological trade-off of photoperiod sensitivity to a quantifiable measure of performance stability, underscoring the critical importance of phenology as a target trait for breeding. Consequently, the framework provides a powerful tool for developing more targeted selection strategies, enabling the precise deployment of hybrids based on their predicted phenological response to specific mega-environments, thereby optimizing resource allocation and accelerating genetic gain.

ACKNOWLEDGMENTS

This research was supported by the Coordination for the Improvement of Higher Education Personnel (CAPES) and São Paulo State Research Support Foundation (FAPESP, Grant 2024/01868-9 and 2025/11161-2), National Council for Scientific and Technological Development (CNPq) and Luiz de Queiroz College of Agriculture of the University of São Paulo.

DATA AVAILABILITY

The datasets generated and/or analyzed during the current research are available from the corresponding author upon reasonable request.

REFERENCES

Araújo MS, Chaves SF, Dias LA, Ferreira FM, Pereira GR, Bezerra AR, Alves RS, Heinemann AB, Breseghello F, Carneiro PC and Krause MD (2024) GIS-FA: An approach to integrating thematic maps, factor-analytic, and envirotyping for cultivar targeting. **Theoretical and Applied Genetics 137**: 80.

Araújo MS, Pavan JPS, Stella AA, Fregonezi BF, Lima NF, Leles EP, Santos MF, Goldsmith P, Chigeza G, Diers BW and Pinheiro JB (2025) Optimizing soybean variety selection for the Pan-African trial network using factor analytic models and envirotyping. **Frontiers in Plant Science 16**: 1594736.

Butler DG, Cullis BR, Gilmour AR, Gogel BJ and Thompson RA (2023) **ASReml-R reference manual version 4**. VSN International Ltd, Hemel Hempstead, 183p.

Caliński T and Harabasz J (1974) A dendrite method for cluster analysis. **Communications in Statistics-theory and Methods 3**: 1-27.

Cooper M and DeLacy IH (1994) Relationships among analytical methods used to study genotypic variation and genotype-by-environment interaction in plant breeding multi-environment experiments. **Theoretical and Applied Genetics 88**: 561-572.

Cooper M, Messina CD, Tang T, Gho C, Powell OM, Podlich DW, Technow F and Hammer GL (2022) Predicting genotype × environment × management (G×E×M) interactions for the design of crop improvement strategies: integrating breeder, agronomist, and farmer perspectives. **Plant Breeding Reviews 46**: 467-585.

Costa-Neto G, Crossa J and Fritsche-Neto R (2021a) Enviromic assembly increases accuracy and reduces costs of the genomic prediction for yield plasticity in maize. **Frontiers in Plant Science 12**: 717552.

Costa-Neto G, Galli G, Carvalho HF, Crossa J and Fritsche-Neto R (2021b) EnvRtype: a software to interplay enviromics and quantitative genomics in agriculture. **G3: Genes, Genomes, Genetics 11**: p.jkab040.

Crossa J, Yang RC and Cornelius PL (2004) Studying crossover genotype × environment interaction using linear-bilinear models and mixed models. **Journal of Agricultural, Biological, and Environmental Statistics 9**: 362-380.

Cruz DD, Heinemann AB, Marcatti GE and Resende RT (2025) Defining the target population of environments (TPE) for enviromics studies using R-based GIS tools. **Crop Breeding and Applied Biotechnology 25**: e50822519.

Drouault J, Palaffre C, Millet EJ, Rodriguez J, Martre P, Johnson K, Parent B, Welcker C and Wisser RJ (2025) A reaction norm for flowering time plasticity reveals physiological footprints of maize adaptation. **G3: Genes, Genomes, Genetics 15**: jkaf095.

Falconer DS and Mackay TFC (1996) **Introduction to quantitative genetics**. Longman, Essex, 438p.

FAO - Food and Agriculture Organization of the United Nations (2025) Global agro-ecological zones (GAEZ) Available at <https://gaez.fao.org/>. Accessed on: October 20, 2025.

Genomes to Fields (2025) **Genomes to fields 2024 maize genotype by environment prediction competition**. Available at <https://www.maizegxeprediction.org/>. Accessed on July 15, 2025.

He K, Yu T, Gao S, Chen S, Li L, Zhang X, Huang C, Xu Y, Wang J, Prasanna BM and Hearne S (2025) Leveraging automated machine learning for environmental data-driven genetic analysis and genomic prediction in maize hybrids. **Advanced Science 12**: 2412423.

Huehn M (1990) Nonparametric measures of phenotypic stability. Part 1: Theory. **Euphytica 47**: 189-194.

Jarquín D, Crossa J, Lacaze X, Du Cheyron P, Daucourt J, Lorgeou J, Piraux F, Guerreiro L, Pérez P, Calus M and Burgueño J (2014) A reaction norm model for genomic selection using high-dimensional genomic and environmental data. **Theoretical and Applied Genetics 127**: 595-607.

Lopez-Cruz M, Aguate FM, Washburn JD, Leon N, Kaeppler SM, Lima DC, Tan R, Thompson A, La Bretonne LW and Los Campos G (2023) Leveraging data from the Genomes-to-Fields Initiative to investigate genotype-by-environment interactions in maize in North America. **Nature Communications 14**: 6904.

Pereira GR, Araújo MS, Chaves SFS, Blasques GM, Dias LAS, Silva FL, Bezerra ARG, Carneiro PCS and Dias KOG (2025) Exploring genotype-by-environment interactions in tropical soybean multi-environment trials. **Euphytica 221**: 221.

Resende RT, Piepho HP, Rosa GJ, Silva-Junior OB, Silva FF, Resende MDV and Grattapaglia D (2021) Enviromics in breeding: Applications and perspectives on envirotypic-assisted selection. **Theoretical and Applied Genetics 134**: 95-112.

Smith A, Cullis B and Thompson R (2001) Analyzing variety by environment

data using multiplicative mixed models and adjustments for spatial field trend. **Biometrics 57**: 1138-1147.

Smith AB and Cullis BR (2018) Plant breeding selection tools built on factor analytic mixed models for multi-environment trial data. **Euphytica 214**: 143.

Smith AB, Cullis BR and Thompson R (2005) The analysis of crop cultivar breeding and evaluation trials: an overview of current mixed model approaches. **The Journal of Agricultural Science 143**: 449-462.

Wang Y, Huang H, Rudin C and Shaposhnik Y (2021) Understanding how dimension reduction tools work: an empirical approach to deciphering t-SNE, UMAP, TriMAP, and PaCMAP for data visualization. **Journal of Machine Learning Research 22**: 1-73.